

# Colorimetric Polydiacetylene–Aerogel Detector for Volatile Organic Compounds (VOCs)

Susmita Dolai,<sup>†</sup> Susanta Kumar Bhunia,<sup>†</sup> Stella S. Beglaryan,<sup>§</sup> Sofiya Kolusheva,<sup>‡</sup> Leila Zeiri,<sup>‡</sup> and Raz Jelinek<sup>\*,†,‡,§</sup>

<sup>†</sup>Department of Chemistry, Ben Gurion University of the Negev, Beer Sheva 84105, Israel

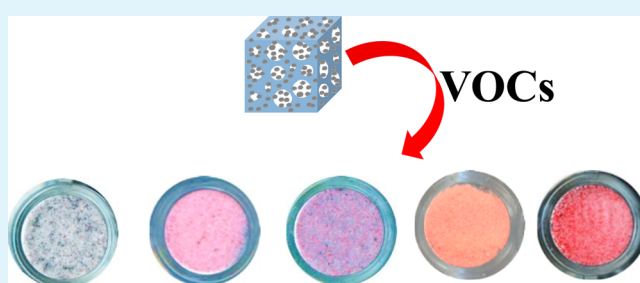
<sup>‡</sup>Ilse Katz Institute for Nanotechnology, Ben Gurion University of the Negev, Beer Sheva 84105, Israel

<sup>§</sup>Chemistry Department “G. Ciamician”, Green Chemistry Lab, University of Bologna, Via S. Alberto 163, 48100 Ravenna, Italy

## Supporting Information

**ABSTRACT:** A new hybrid system comprising polydiacetylene (PDA), a chromatic conjugated polymer, embedded within aerogel pores has been constructed. The PDA–aerogel powder underwent dramatic color changes in the presence of volatile organic compounds (VOCs), facilitated through infiltration of the gas molecules into the highly porous aerogel matrix and their interactions with the aerogel-embedded PDA units. The PDA–aerogel composite exhibited rapid color/fluorescence response and enhanced signals upon exposure to low VOC concentrations. Encapsulation of PDA derivatives displaying different headgroups within the aerogel produced distinct VOC-dependent color transformations, forming a PDA–aerogel “artificial nose”.

**KEYWORDS:** polydiacetylene, aerogel, volatile organic compounds, colorimetric sensors, nanoporous materials



## INTRODUCTION

Volatile organic compounds (VOCs) might be harmful to human health, and exposure to such vapors is considered hazardous and associated with varied pulmonary diseases.<sup>1–4</sup> Detection of VOCs is thus essential for early warning, monitoring of occupational hazards, and security applications. Varied techniques are currently employed for VOC detection and analysis, including gas chromatography–mass spectrometry,<sup>5</sup> surface acoustic wave sensors,<sup>6</sup> chemiresistor-based sensing,<sup>2</sup> and others.<sup>7,8</sup> Despite the versatility of detection methods, however, current technologies are generally limited in term of practical, easy-to-apply VOC sensing due to complexity and elaborate synthesis of the gas adsorption and/or transduction substances, high cost of the devices, and insufficient sensitivity/selectivity.

Identification of host materials capable of adsorption of VOCs is a fundamental requisite of effective sensing platforms. Aerogels, among the lowest density solid materials, have been employed in vapor sensor designs.<sup>3,9–12</sup> Aerogels have been produced from diverse building blocks, comprising scaffolding of silicon,<sup>13</sup> carbon,<sup>14</sup> metals,<sup>15</sup> metal oxides,<sup>16</sup> organic polymers,<sup>17</sup> and others. Hydrophobic silica aerogels, in particular, exhibit pronounced porous structures with very high internal surface area available for adsorption of guest molecules.<sup>9</sup> Silica aerogels have been employed as insulation substances in the aerospace industry,<sup>18</sup> sorption of miscible organic solvents in water,<sup>9</sup> and sensing of air pollutants.<sup>3</sup> While silica aerogels are excellent gas adsorbents, the main challenge in using them for

VOC sensing concerns the identity of signal transduction elements. A recent study has reported encapsulation of fluorescent carbon dots within aerogel pores and use of the hybrid matrix for aromatic VOC sensing.<sup>4</sup>

Here we report on a new VOC detection system comprising aerogel associated with polydiacetylene (PDA). PDA constitutes a class of conjugated polymers exhibiting unique color and fluorescence properties.<sup>19–25</sup> In particular, numerous reports have demonstrated dramatic visible colorimetric transformations of PDA assemblies, induced by varied external stimuli and analytes.<sup>19,20,26–32</sup> While almost all published studies thus far have employed PDA systems in solution environments, few reports described applications of the polymer for gas sensing.<sup>19,33,34</sup> Published PDA-based assemblies for VOC detection, however, are synthetically complex and/or exhibit limited sensing parameters, e.g., slow response time and low sensitivity.<sup>19</sup>

This paper presents a new hybrid PDA–aerogel, produced through a simple single-step method. The PDA–aerogel was employed for VOC detection and exhibits excellent sensitivity and rapid colorimetric/fluorescence response. Importantly, the chromatic transformations of the PDA–aerogel were VOC-dependent, reflecting the distinct interactions of the VOC molecules with the aerogel-embedded PDA. Furthermore,

**Received:** November 11, 2016

**Accepted:** December 28, 2016

**Published:** December 28, 2016

“color fingerprinting” of VOCs was demonstrated by encapsulating in the aerogel matrix PDAs displaying different molecular headgroups. Overall, the PDA–aerogel matrix could be used as a platform for detection, visualization, and speciation of VOCs.

## ■ EXPERIMENTAL SECTION

**Materials.** Tetraethylorthosilicate (TEOS) was purchased from Sigma-Aldrich, USA. The diacetylene monomer 10,12-tricosadiynoic acid (TRCDA) was purchased from Alfa-Aesar, England. Tetrahydrofuran (THF) and diethyl ether were purchased from Bio-Lab Ltd. Dichloromethane (DCM), ammonium hydroxide (NH<sub>4</sub>OH), chloroform (CHCl<sub>3</sub>), methanol, dimethylformamide (DMF), and acetone were purchased from Frutarom Ltd. (Haifa, Israel). Benzene was purchased from Merck. Lauroyl chloride was bought from TCI, Japan. Chloroform, toluene, pentane, and *n*-hexane were purchased from Daejung Chemicals, Korea. Ethanol was purchased from J. T. Baker. Tetrahydrofuran was purchased from Acros Organics, USA. Ethyl acetate and concentrated hydrochloric acid (HCl) were purchased from Bio-Lab Ltd. (Jerusalem, Israel). 2-Propanol was bought from SDFCL, India. All the reagents and solvents were used as received without further purification.

**Aerogel Synthesis.** Wet silica gel was prepared according to previous report.<sup>3,4</sup> Briefly, 5 mL of TEOS, 15 mL of anhydrous ethanol (EtOH), 5 mL of distilled water, and 5 μL of concentrated hydrochloric acid were mixed in a 100 mL flask and stirred in a 60 °C water bath for 90 min. Subsequently, 25 mL of ethanol, 13 mL of distilled water, and 15 μL of NH<sub>4</sub>OH were added to the solution and stirred for 30 min under the same temperature. The prepared wet silica gel was coated with parafilm before it was further dried and transferred into 200 mL of anhydrous ethanol and placed in GCF1400 atm furnace under ultrapure N<sub>2</sub> gas atmosphere. Afterward, the outlet was closed while the ultrapure N<sub>2</sub> was continuously passed into the autoclave and reached 1 MPa. The temperature was first raised quickly from room temperature to 200 °C, increased slowly to 246 °C, followed by 260 °C for 3 h at 2 MPa N<sub>2</sub> gas pressure. Finally, the white colored silica aerogel were obtained after opening the autoclave.

**Diacetylene Monomers Synthesis.** 10,12-Tricosadiyn Amine (TR-NH<sub>2</sub>). Synthesis of 10,12-tricosadiyn amine was carried out through a two-step pathway.<sup>20</sup> Briefly, 570 mg of TRCDA was dissolved in 20 mL of DCM. Then 2 mL of oxalyl chloride was added into TRCDA solution under an argon atmosphere. Several drops of DMF were then added as catalyst followed by stirring overnight at room temperature. Then solvent was evaporated, and the residue was dissolved in dry THF (20 mL). The solution was then slowly added to 30 mL of NH<sub>4</sub>OH (25%) in an ice bath and stirred overnight. The solvent was evaporated, and the residue was purified and added to 30 mL of diethyl ether. LiAlH<sub>4</sub> (550 mg) was added to it while keeping the solution in an ice bath under overnight stirring and then poured into a saturated solution of NH<sub>4</sub>Cl. The aqueous layer was then extracted with ethyl acetate. The combined organic layer was washed with saturated NaCl solution and then dried with MgSO<sub>4</sub>, filtered, and evaporated. The residue was purified with column chromatography over silica gel. Synthesis scheme has been shown in Supporting Information, Figure S1.

**Methyl Tricoso-10,12-diynoylphenylalaninate (TR-MPhe).** Methyl tricoso-10,12-diynoylphenylalaninate (TR-MPhe) was synthesized according to published protocols.<sup>35</sup> Phenylalanine (3 mmol) and trimethylsilyl chloride (6 mmol) are stirred in MeOH (10 mL) at rt for 24 h. The solvent was evaporated under reduced pressure, and the crude (MPhe\*HCl) was used with TR-NHS without further purifications. TRCDA (0.29 mmol) was solubilized in DCM (3 mL). *N*-Hydroxysuccinimide (0.35 mmol) and 1-ethyl-3-(3-dimethylamino)propyl)carbodiimide (0.55 mmol) were solubilized in DCM (5 mL) and mixed to the solution of TRCDA under stirring at room temperature. After 20 h, the solvent was evaporated under reduced pressure followed by extraction from water with diethyl ether. The organic layers were recovered, dried with anhydrous Na<sub>2</sub>SO<sub>4</sub>, filtered, and evaporated to get TR-NHS and dissolved in DCM.

MPhe\*HCl (0.49 mmol) was added to the mixture followed by dropwise addition of triethylamine (0.29 mmol) with stirring for 24 h. Then the product was purified by column chromatography. Synthesis scheme is shown in Supporting Information, Figure S2.

**Synthesis of PDA–Aerogel.** PDA–aerogel was fabricated by different techniques using different TRCDA derivatives. First, 570 mg of TRCDA was dissolved in 20 mL of DCM. Then the solution was filtered through a membrane filter (Millex, Nylon, 0.45 μm). Then 20 μL of the filtered TRCDA solution was drop-casted on 10 mg of aerogel powder. Then the TRCDA–aerogel was irradiated with ultraviolet light (254 nm) for 0.5 min to produce the polymerized, blue phase of polydiacetylene. TRCDA and TR-NH<sub>2</sub> or TR-MPhe mixtures were mixed at 5:1 ratio in the case of diacetylene derivative mixtures.

**VOC Sensing.** Predetermined quantities of organic liquids were placed in a 500 mL closed glass container to obtain desired vapor pressures using a MiniRAE Lite (PID). In parallel, 50 mg of PDA–aerogel was placed in the sealed container and incubated prior to colorimetric and fluorescence analysis (Supporting Information, Figure S3).

**Instrumentation and Characterization.** Scanning electron microscopy (SEM) experiments were conducted using a JEOL (Tokyo, Japan) model JSM-7400F scanning electron microscope. Images were taken after sputtering a thin film of gold over the substrates for better contrast and minimum charging. Fluorescence emission spectra of the PDAs–aerogel were recorded on a Varioskan plate reader using 482 nm excitation wavelength. Confocal microscopy images of PDAs–aerogel were acquired on an UltraVIEW system (PerkinElmer Life Sciences, Waltham, MA) equipped with an Axiovert-200 M microscope (Zeiss, Oberkochen, Germany) and a Plan-Neofluar 63×/1.4 oil objective. The excitation wavelength at 488 nm was produced by an argon/krypton laser. Emitted light was passed through a barrier filter (580–700 nm). Surface area, pore volume, and pore diameters of the PDA–aerogel were measured by a BET instrument (Quantachrome High Speed gas sorption analyzer NOVA-1200e). Degassing of the PDA–aerogel was carried out for 21 h in order to evaporate all traces of solvents and moisture followed by N<sub>2</sub> adsorption–desorption in liquid nitrogen.

Raman spectra were recorded with a Horiba–Jobin–Yvon LabRam HR 800 micro-Raman system, equipped with a Synapse CCD detector. The excitation source was an He–Ne laser (633 nm), with a power of 5 mW. To protect the samples the laser power was reduced by 1000 using ND filters. The laser was focused with x100× long-focal-length objective to a spot of about 1 μm. Measurements were taken with the 600 g mm<sup>-1</sup> grating and a confocal hole of 100 μm with a typical exposure time of 1 min.

**Chromatic (Red–Green–Blue, RGB) Analysis.** Multiwell plates containing multicolored dust PDA–aerogel were scanned in transmitted mode on an Epson 4990 photo scanner to produce 2400 dpi, 24-bit color depth red–green–blue (RGB) images. Digital colorimetric analysis (DCA) was performed by extracting RGB channels values for each pixel within the sample spots in the scanned images, and the color change values were estimated using Matlab R2010 scientific software (The Mathworks, Inc., MA, USA). Briefly, DCA handles the standard “red–green–blue” (sRGB) model, essentially translating every color signal into three distinct values corresponding to the intensities of red (R), green (G), and blue (B) color channels. Accordingly, the relative intensity of a particular RGB component in a scanned image can be described as the chromaticity level. For example, the red chromaticity level (*r*) in each pixel was figured as

$$r = R/(R + B + G)$$

where R (red), G (green), and B (blue) are the three primary color components. For a defined surface area within a PDA-based sensor well, we classified a quantitative parameter denoted chromatic response that represents the total blue–red transformations of the pixels encompassed in the area,

$$\%RGB = (r_{\text{sample}} - r_0)/(r_{\text{max}} - r_0) \times 100\%$$

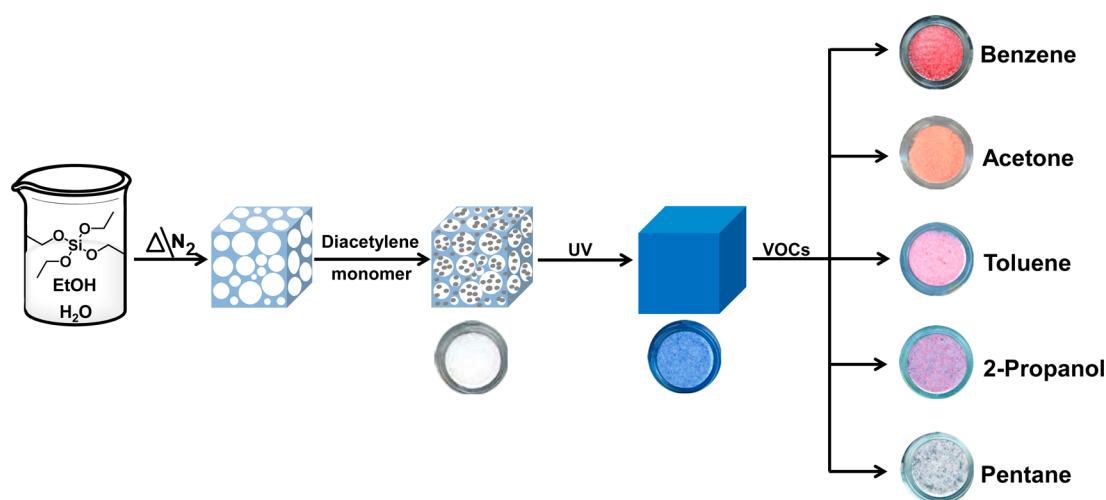


**Figure 1.** Synthesis of the polydiacetylene (PDA)–aerogel and its colorimetric properties. Schematic illustration of PDA–aerogel fabrication. The circled digital photographs depict the visible colors generated following exposure to different VOCs (concentrations 1000 ppm).

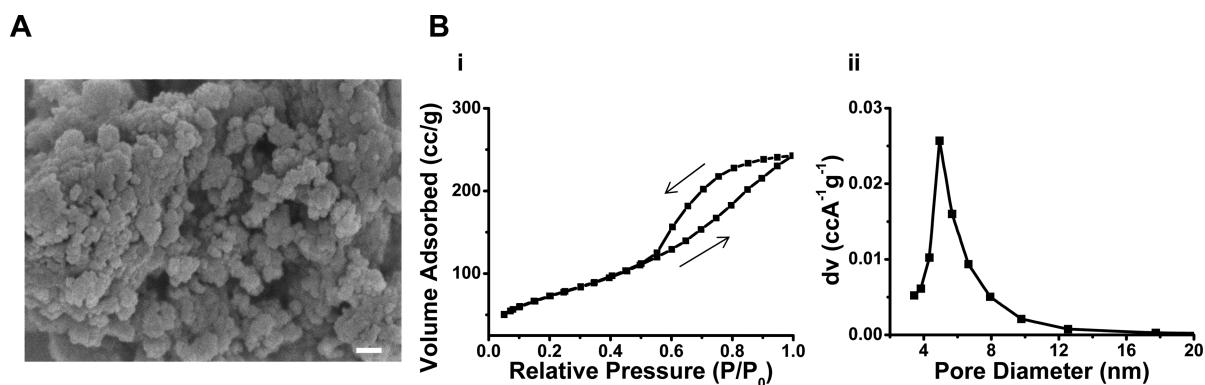


**Figure 2.** Characterization of the PDA–aerogel. (A) Scanning electron microscopy (SEM) image of the PDA/aerogel surface. The scale bar corresponds to 100 nm. (B) BET analysis: (i)  $N_2$  adsorption–desorption isotherms of PDA/aerogel; (ii) pore size distribution curve indicating average pore diameter of 4.93 nm.

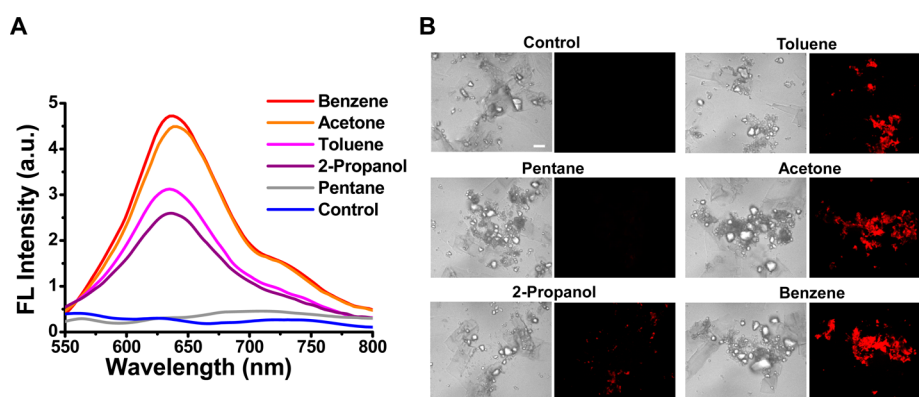


**Figure 3.** Fluorescence analysis of PDA–aerogel upon exposure to different volatile organic compounds (VOCs). (A) Fluorescence emission spectra (excitation 482 nm) of PDA–aerogel following 60 min exposure to different VOCs (1000 ppm concentrations). (B) Confocal fluorescence microscopy images (excitation 488 nm) of PDA–aerogel after 60 min exposure to different VOCs. Scale bar corresponds to 10  $\mu$ m.

where  $r_{\text{sample}}$  is the average red chromaticity level of all pixels in the scanned surface,  $r_0$  is the average red level calculated in a blank surface (blue sensor well), and  $r_{\text{max}}$  is the average red chromaticity level of the maximal blue–red transition, an area of the sensor well in which the most pronounced blue–red transition was induced (positive control). In essence, the calculated %RGB is the normalized change in the red chromaticity level within the sensor well surface on which the tested sample was deposited.

## RESULTS AND DISCUSSION

The simple preparation scheme of the polydiacetylene (PDA)–aerogel hybrid and representative VOC-induced color transformations are shown in Figure 1. The porous aerogel framework was first generated through high temperature silica annealing in the presence of pressurized nitrogen gas.<sup>36</sup> Following aerogel formation, the PDA precursor (10,12-

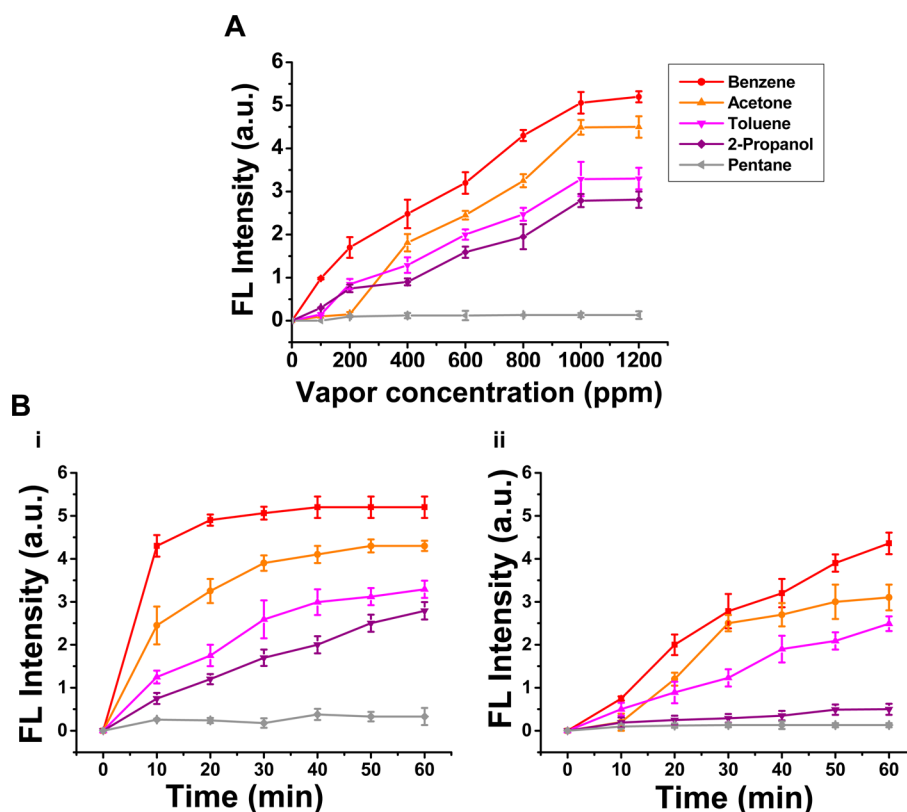


**Figure 4.** VOC-induced fluorescence emissions of PDA-aerogel. Fluorescence titration curves (A) and fluorescence kinetics (B) (excitation 482 nm, emission 635 nm) recorded in PDA-aerogel (i) and silica gel (ii) upon exposure to VOCs at concentrations of 1000 ppm.

tricosadinoic acid, TRCDA) was drop-casted on the aerogel powder. The TRCDA monomers were efficiently adsorbed and immobilized upon the hydrophobic domains within the aerogel pores.<sup>9</sup> Irradiation of the TRCDA/aerogel construct with ultraviolet (UV) light induced polymerization of the aerogel-embedded TRCDA monomers, generating the blue-phase conjugated polydiacetylene (PDA). Importantly, the blue PDA appeared uniformly distributed within the aerogel powder, likely due to the high porosity of the aerogel. Figure 1 also illustrates the dramatic color transformations of the blue PDA/aerogel induced by exposure to different VOCs; notably, the photographs shown in Figure 1 (right) demonstrate that distinct VOC-dependent colors were generated.

Characterization of the structural and physical properties of the hybrid PDA/aerogel was carried out (Figure 2). The representative scanning electron microscopy (SEM) image of the PDA/aerogel in Figure 2A is similar to the bare aerogel, displaying the typical hierarchical organization exhibiting high-surface area.<sup>3</sup> The Brunauer-Emmett-Teller (BET) analysis in Figure 2B indicates a relatively high specific surface area (265 m<sup>2</sup>/g) suitable for adsorption of gas molecules. Specifically, the isotherms in Figure 2B,i exhibit type IV adsorption with a distinct hysteresis loop.<sup>37</sup> Figure 2B,ii further reveals high pore volume (0.34 cc/g) and sizable pore diameter (4.93 nm) of the PDA/aerogel. Overall, the BET analysis in Figure 2 underscores the high porosity of the PDA-aerogel and its applicability for efficient vapor adsorption.

Figures 3–6 illustrate application of the PDA/aerogel construct for sensing volatile organic compounds (VOCs). Figure 3 depicts spectroscopic and microscopic fluorescence analysis of the PDA-aerogel upon incubation with different VOCs, all applied at the same concentration (1000 ppm).

Figure 3A reveals significantly different fluorescence emissions (excitation 482 nm) of the PDA-aerogel generated by the VOCs. Notably, the relative fluorescence emission intensities shown in Figure 3A echo the colorimetric transitions (Figure 1); previous studies similarly reported a direct correlation between the extent of blue-red transformations of PDA systems and the degree of fluorescence emission.<sup>20</sup> Accordingly, benzene and acetone vapors, which produced red and orange PDA-aerogels (Figure 1), gave rise to the most pronounced fluorescence emission (Figure 3A). Toluene and 2-propanol, which induced blue-purple transitions upon incubation with the PDA-aerogel (Figure 1) generated lower PDA fluorescence compared to benzene and acetone (Figure 3A), and pentane essentially gave rise to flat fluorescence emission (Figure 3A), reflecting the apparent quenching of PDA blue color by this vapor (Figure 1).

The confocal microscopy images of the PDA-aerogel particulates presented in Figure 3B complement the fluorescence spectroscopy measurements and highlight the distinct VOC-induced fluorescence transformations. Specifically, Figure 3B reveals different intensities of PDA-aerogel particles, depending upon the VOCs applied. Similar to the fluorescence results in Figure 3A, Figure 3B demonstrates that benzene and acetone induced the most fluorescently intense PDA-aerogel particulates, less fluorescent particles are apparent after exposure to toluene and 2-propanol, and no fluorescent particle were recorded upon exposure of the PDA-aerogel to pentane vapor.

Figure 4 highlights the sensitivity and fast chromatic response of the PDA-aerogel upon VOC exposure, and the contribution of the aerogel matrix to the unique chromatic properties of the hybrid material. Figure 4A presents fluorescence titration curves

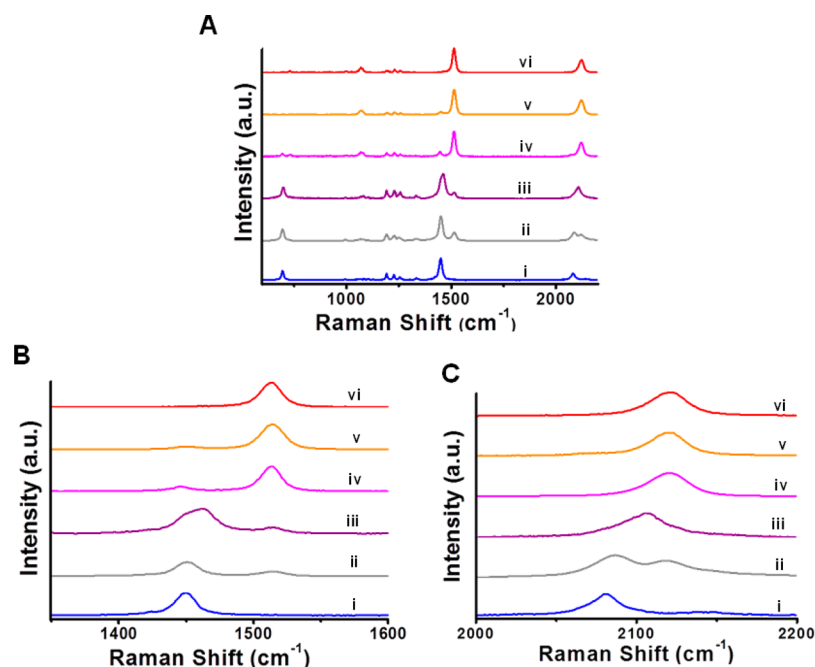


**Figure 5.** Raman spectra of PDA–aerogel. (A) Full spectral range; (B,C) magnified regions. (i) control; (ii) pentane; (iii) 2-propanol; (iv) toluene; (v) acetone; (vi) benzene. (B,C) Magnified images corresponding to the carbon–carbon double bond and carbon–carbon triple bond regions, respectively.

(excitation at 482 nm, emission at 635 nm) recorded upon exposure of the PDA–aerogel to different VOC concentrations. As apparent in Figure 4A, the detection thresholds for VOCs tested were between 100 and 200 ppm; this sensitivity is significantly better than previously reported PDA-based vapor sensors.<sup>19</sup>

Comparison of the fluorescence kinetic data of PDA–aerogel (Figure 4Bi) and PDA embedded within conventional silica gel matrix (Figure 4Bii) reveals faster and more pronounced fluorescence response upon VOC exposure of PDA–aerogel. This result points to the significance of the aerogel framework to the sensing performance; the pronounced porosity of the aerogel likely promoted adsorption of the guest vapor molecules, giving rise to the rapid chromatic response upon interactions with the pore-associated PDA. It should be also noted that chromatic image analysis<sup>38</sup> (Supporting Information, Figure S4) yielded a similar kinetic profile as the fluorescence experiments depicted in Figure 4, underscoring the versatility of chromatic transformation detection methods (e.g., fluorescence emission or color change).

To account for the distinct VOC-induced chromatic transformations of the PDA–aerogel, we carried out Raman scattering analysis (Figure 5). Raman spectroscopy has been applied in numerous studies for characterization of the structural/photophysical transformations of PDA assemblies.<sup>39–44</sup> In particular, Raman scattering experiments shed light on the molecular features of chromatically transformed PDA, through analysis of the shifts and intensities of the spectral peaks at around 1500  $\text{cm}^{-1}$  (carbon–carbon double bond region) and 2100  $\text{cm}^{-1}$  (carbon–carbon triple bond).<sup>39,40</sup> Indeed, the relationships between the intensities of the Raman peaks corresponding to the *blue* PDA at 1450 and 2080  $\text{cm}^{-1}$ , and red-phase PDA at 1515 and 2120  $\text{cm}^{-1}$ , respectively, illuminate the VOC-induced chromatic transitions and relate these transitions to structural features of the PDA units. Specifically, the vapors of both *benzene* (Figure 5,vi) and *acetone*

(Figure 5,v) gave rise to Raman signals ascribed to red-phase PDA,<sup>40</sup> consistent with the pronounced color and fluorescence transformations induced by these VOCs (Figures 1 and 3, respectively). Figure 5,iv reveals that *toluene* similarly generated Raman spectral shifts associated with red-phase PDA. Interestingly, the Raman signature of 2-propanol vapor (Figure 5,iii), featuring Raman peaks at 1460 and 2105  $\text{cm}^{-1}$ , indicates formation of a *purple*, intermediate PDA phase.<sup>40,45</sup>

The variations of chromatic response (Figures 3 and 4) and Raman scattering data (Figure 5) likely correspond to different interactions of the VOCs with the PDA headgroup. Specifically, the amphiphilic nature of PDA, e.g., the polar headgroup and hydrophobic side chains, dictates that *polarity* and *hydrophobicity* of the target analyte constitute the primary factors affecting the degree of chromatic transformations.<sup>19,40,46,47</sup> The interplay between these two parameters, however, might be complex. Acetone, for example, which is highly polar, induced a similar chromatic transition (Figures 3 and 4) and Raman shift (Figure 5) as benzene, which is apolar. Interestingly, 2-propanol, which is also polar,<sup>48</sup> gave rise to only a mild chromatic transformation (Figures 3 and 4). This observation might be ascribed to the strong affinity between alcohols and the carboxylic moieties of PDA.<sup>49</sup> Such interactions have been shown to stabilize the intermediate purple state of PDA.<sup>41</sup>

To explore application of the new PDA–aerogel platform for distinguishing among different vapors, we recorded the color transitions induced by VOCs in aerogels embedding PDA that was produced from monomers displaying different headgroups (Figure 6). Numerous studies have shown that modulation of the PDA headgroups exerted significant effects upon the chromatic properties of PDA systems and the color transformations.<sup>20,28,50</sup> Figure 6A depicts the chemical structures of the three diacetylene monomers employed. The commercially available diacetylene monomer (compound 1) displays carboxylic moieties, the amine-functionalized 2 exhibits a more polar headgroup, while 3 was functionalized with bulky,

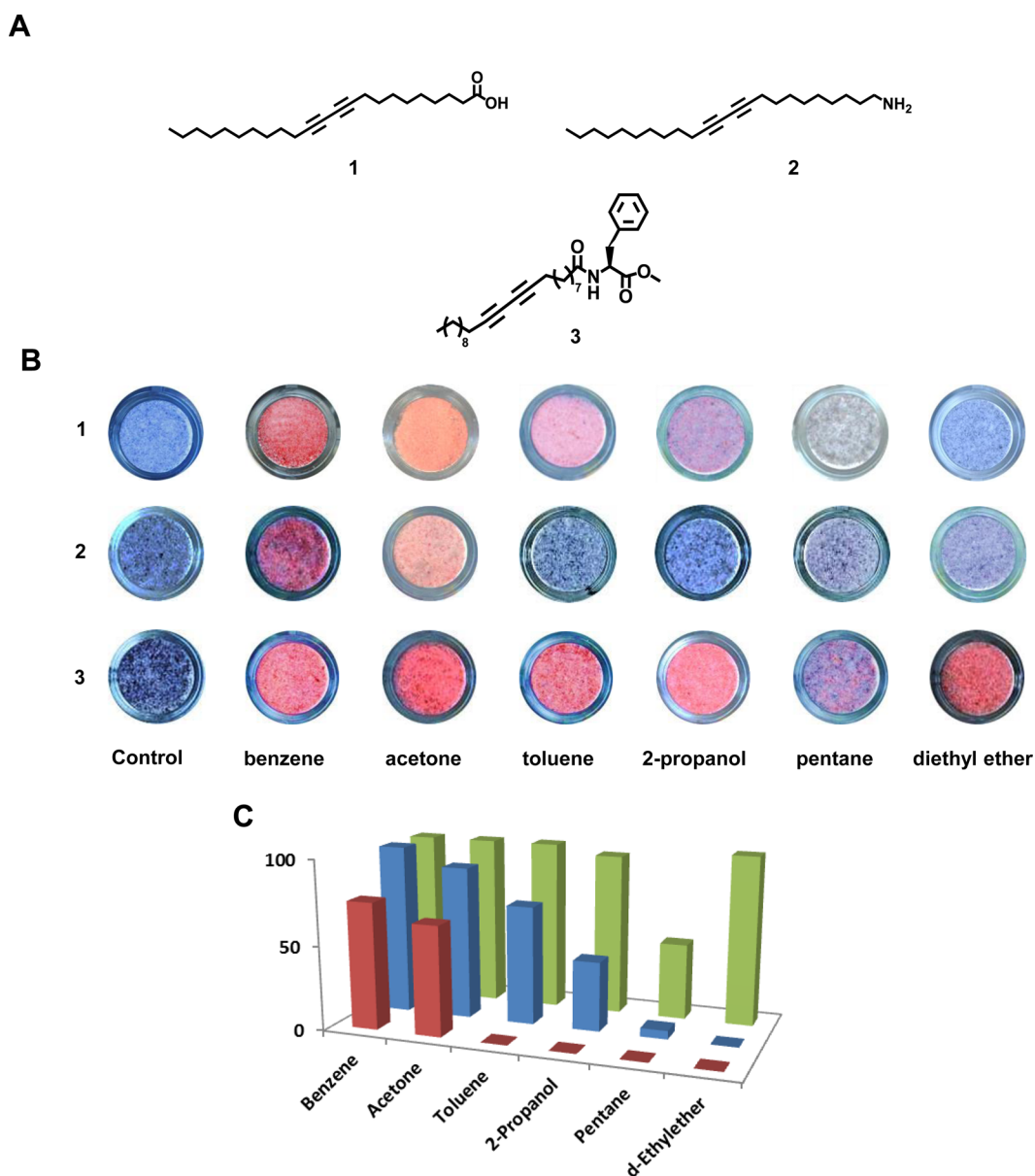


**Figure 6.** “Color fingerprinting” of VOCs using aerogel-embedded PDA derivatives. (A) Structures of the monomers employed; (B) scanned photographs of the PDA-aerogels after 60 min exposure to the VOCs (concentrations 1000 ppm); (C) chromatic (Red, Blue, Green: RGB) analysis<sup>38</sup> of the recorded color responses depicted in (B). Height of the bars indicate more pronounced blue–red transformations. Red bars, 1; blue, 2; green, 3.

hydrophobic phenyl residues. The scanned photographs in Figure 6B and corresponding chromatic red–green–blue (RGB) signals<sup>38</sup> in Figure 6C demonstrate significant variability in color transformations induced by the VOCs, which clearly depended upon the different embedded PDA.

Interestingly, Figure 6B indicates that the aerogel hybrid embedding the MPhe–PDA derivative (e.g., monomer 3) produced much more pronounced blue–red transformations compared to the two other PDA derivatives. This result is ascribed to the hydrophobicity of the phenyl moieties exhibiting greater interactions with the aerogel-adsorbed VOC molecules. The different blue–red transformations induced in 3–aerogel by specific VOCs point to the significance of headgroup–analyte interactions in determining the extent of color change. For example, the more pronounced red color induced by benzene compared to *n*-pentane (Figure 6B) is

likely ascribed to the high affinity between the benzene and phenyl rings; the corresponding interaction between the pentane hydrocarbon chain and the headgroup of 3 is expected to be less pronounced.

1–aerogel and 2–aerogel hybrids exhibited somewhat similar VOC-induced colors which were less significant than 3–aerogel (Figure 6B, top rows), likely reflecting the polarities of their headgroups. Color differences were apparent between 1–aerogel and 2–aerogel, however, for most VOCs examined, confirming the roles of the PDA headgroup moieties as fundamental determinants of the colorimetric transformations. Distinctive color transformations were also recorded upon examination of two closely-related VOCs such as ethanol and 2-propanol (Figure S5). Overall, the PDA–aerogel color matrix in Figure 6B and the corresponding RGB pattern in Figure 6C provide compelling evidence for the feasibility of VOC

“fingerprinting” through array-based pattern recognition methods, in which each array element comprised of a different PDA derivative. PDA array-based sensing strategies have been reported.<sup>19,35</sup> Powerful pattern-recognition methods for VOC detection have been also developed.<sup>51</sup>

## CONCLUSIONS

We constructed a VOC sensor comprising PDA within the porous framework of a silica aerogel. The structural and physical properties of both the aerogel matrix and embedded PDA were retained following the fabrication procedure. The PDA–aerogel hybrid was used as a sensor for different VOCs, exploiting the porosity and high surface area for adsorption of the volatile compounds and their effects upon both the PDA color and fluorescence. Importantly, the observed chromatic modulation was dependent upon the electronic, structural features, and particularly the polarity of the VOCs. Accordingly, the PDA–aerogel vapor sensor could distinguish among different VOCs. The PDA–aerogel sensor exhibits notable practical advantages. Preparation of the hybrid material is straightforward, using inexpensive and readily available reagents. The actual sensing experiments are easy to perform and carried out through visible color transformations that could be also quantified using spectrophotometry.

## ASSOCIATED CONTENT

### Supporting Information

The Supporting Information is available free of charge on the ACS Publications website at DOI: 10.1021/acsami.6b14469.

Synthesis scheme of monomers preparation, schematic diagram of the experimental setup for VOC sensing, color transformation titrations of PDA–aerogel in the presence of different concentrations of different VOCs, and distinctive color transformations using closely-related VOCs (PDF)

## AUTHOR INFORMATION

### Corresponding Author

\*E-mail: razj@bgu.ac.il.

### ORCID

Raz Jelinek: 0000-0002-0336-1384

### Notes

The authors declare no competing financial interest.

## ACKNOWLEDGMENTS

Dr. Susanta Kumar Bhunia is grateful to the Planning and Budgeting Committee (PBC) of the Israeli Council for Higher Education for an Outstanding Postdoctoral Fellowship. We thank Xiuxiu Yin and Dr. Nagappa L. Teradal for SEM experiments.

## REFERENCES

- (1) Konvalina, G.; Haick, H. Sensors for Breath Testing: From Nanomaterials to Comprehensive Disease Detection. *Acc. Chem. Res.* **2014**, *47*, 66–76.
- (2) Kim, J. S.; Yoo, H. W.; Choi, H. O.; Jung, H. T. Tunable Volatile Organic Compounds Sensor by Using Thiolated Ligand Conjugation on MoS<sub>2</sub>. *Nano Lett.* **2014**, *14*, 5941–5947.
- (3) Wang, R. X.; Li, G. L.; Dong, Y. Q.; Chi, Y. W.; Chen, G. N. Carbon Quantum Dot-Functionalized Aerogels for NO<sub>2</sub> Gas Sensing. *Anal. Chem.* **2013**, *85*, 8065–8069.
- (4) Dolai, S.; Bhunia, S. K.; Jelinek, R. Carbon-Dot-Aerogel Sensor for Aromatic Volatile Organic Compounds. *Sens. Actuators, B* **2017**, *241*, 607–613.
- (5) Buszewski, B.; Ulanowska, A.; Ligor, T.; Denderz, N.; Amann, A. Analysis of Exhaled Breath from Smokers, Passive Smokers and Non-Smokers by Solid Phase Microextraction Gas Chromatography/Mass Spectrometry. *Biomed. Chromatogr.* **2009**, *23*, 551–556.
- (6) Grate, J. W.; Rose-Pehrsson, S. L.; Venezky, D. L.; Klusty, M.; Wohltjen, M. Smart Sensor System for Trace Organophosphorus and Organosulfur Vapor Detection Employing a Temperature-Controlled Array of Surface Acoustic Wave Sensors Automated Sample Preconcentration, and Pattern Recognition. *Anal. Chem.* **1993**, *65*, 1868–1881.
- (7) Di Natale, C.; Macagnano, A.; Martinelli, E.; Paolesse, R.; D’Arcangelo, G.; Roscioni, C.; Finazzi-Agro, A.; D’Amico, A. Lung Cancer Identification by the Analysis of Breath by Means of an Array of Non-Selective Gas Sensors. *Biosens. Bioelectron.* **2003**, *18*, 1209–1218.
- (8) Turner, C.; Spanel, P.; Smith, D. A Longitudinal Study of Ethanol and Acetaldehyde in the Exhaled Breath of Healthy Volunteers using Selected-Ion Flow-Tube Mass Spectrometry. *Rapid Commun. Mass Spectrom.* **2006**, *20*, 61–68.
- (9) Wang, D.; McLaughlin, E.; Pfeffer, R.; Lin, Y. S. Adsorption of Organic Compounds in Vapor Liquid, and Aqueous Solution Phases on Hydrophobic Aerogels. *Ind. Eng. Chem. Res.* **2011**, *50*, 12177–12185.
- (10) Zuo, L. Z.; Zhang, Y. F.; Zhang, L. S.; Miao, Y. E.; Fan, W.; Liu, T. X. Polymer/Carbon-Based Hybrid Aerogels: Preparation, Properties and Applications. *Materials* **2015**, *8*, 6806–6848.
- (11) Qi, H. S.; Liu, J. W.; Pioteck, J.; Potschke, P.; Mader, E. Carbon Nanotube-Cellulose Composite Aerogels for Vapour Sensing. *Sens. Actuators, B* **2015**, *213*, 20–26.
- (12) Thubsuang, U.; Sukanan, D.; Sahasithiwat, S.; Wongkasemjit, S.; Chaisuwan, T. Highly Sensitive Room Temperature Organic Vapor Sensor Based on Polybenzoxazine-Derived Carbon Aerogel Thin Film Composite. *Mater. Sci. Eng., B* **2015**, *200*, 67–77.
- (13) Li, L. C.; Yalcin, B.; Nguyen, B. C. N.; Meador, M. A. B.; Cakmak, M. Flexible Nanofiber-Reinforced Aerogel (Xerogel) Synthesis Manufacture, and Characterization. *ACS Appl. Mater. Interfaces* **2009**, *1*, 2491–2501.
- (14) Zou, J. H.; Liu, J. H.; Karakoti, A. S.; Kumar, A.; Joung, D.; Li, Q.; Khondaker, S. I.; Seal, S.; Zhai, L. Ultralight Multiwalled Carbon Nanotube Aerogel. *ACS Nano* **2010**, *4*, 7293–7302.
- (15) Kristiansen, T.; Mathisen, K.; Einarsrud, M. A.; Bjorgen, M.; Nicholson, D. G. Single-Site Copper by Incorporation in Ambient Pressure Dried Silica Aerogel and Xerogel Systems: An X-Ray Absorption Spectroscopy Study. *J. Phys. Chem. C* **2011**, *115*, 19260–19268.
- (16) Chervin, C. N.; Clapsaddle, B. J.; Chiu, H. W.; Gash, A. E.; Satcher, J. H.; Kauzlarich, S. M. Aerogel Synthesis of Yttria-Stabilized Zirconia by a Non-Alkoxide Sol-Gel Route. *Chem. Mater.* **2005**, *17*, 3345–3351.
- (17) Boday, D. J.; Stover, R. J.; Muriithi, B.; Keller, M. W.; Wertz, M. W.; DeFriend Obrey, K. A.; Loy, D. A. Strong, Low-Density Nanocomposites by Chemical Vapor Deposition and Polymerization of Cyanoacrylates on Aminated Silica Aerogels. *ACS Appl. Mater. Interfaces* **2009**, *1*, 1364–1369.
- (18) Randall, J. P.; Meador, M. A. B.; Jana, S. C. Tailoring Mechanical Properties of Aerogels for Aerospace Applications. *ACS Appl. Mater. Interfaces* **2011**, *3*, 613–626.
- (19) Eaidkong, T.; Mungkarndee, R.; Phollookin, C.; Tumchareng, G.; Sukwattanasinitt, M.; Wacharasindhu, S. Polydiacetylene Paper-Based Colorimetric Sensor Array for Vapor Phase Detection and Identification of Volatile Organic Compounds. *J. Mater. Chem.* **2012**, *22*, 5970–5977.
- (20) Parambath Kootery, K.; Jiang, H.; Kolusheva, S.; Vinod, T. P.; Ritenberg, M.; Zeiri, L.; Volinsky, R.; Malferrari, D.; Galletti, P.; Tagliavini, E.; Jelinek, R. Poly(methyl methacrylate)-Supported

- Polydiacetylene Films: Unique Chromatic Transitions and Molecular Sensing. *ACS Appl. Mater. Interfaces* **2014**, *6*, 8613–8620.
- (21) Potisatityuenyong, A.; Rojanathanes, R.; Tumcharern, G.; Sukwattanasinitt, M. Electronic Absorption Spectroscopy Probed Side-Chain Movement in Chromic Transitions of Polydiacetylene Vesicles. *Langmuir* **2008**, *24*, 4461–4463.
- (22) Wu, J. C.; Zawistowski, A.; Ehrmann, M.; Yi, T.; Schmuck, C. Peptide Functionalized Polydiacetylene Liposomes Act as a Fluorescent Turn-On Sensor for Bacterial Lipopolysaccharide. *J. Am. Chem. Soc.* **2011**, *133*, 9720–9723.
- (23) Charych, D. H.; Nagy, J. O.; Spevak, W.; Bednarski, M. D. Direct Colorimetric Detection of a Receptor-Ligand Interaction by a Polymerized Bilayer Assembly. *Science* **1993**, *261*, 585–588.
- (24) Koevoets, R. A.; Karthikeyan, S.; Magusin, P. C. M. M.; Meijer, E. W.; Sijbesma, R. P. Cross-Polymerization of Hard Blocks in Segmented Copoly(ether urea)s. *Macromolecules* **2009**, *42*, 2609–2617.
- (25) Pires, A. C. S.; Soares, N. D. F.; da Silva, L. H. M.; da Silva, M. C. H.; Mageste, A. B.; Soares, R. F.; Teixeira, A. V. N. C.; Andrade, N. J. Thermodynamic Study of Colorimetric Transitions in Polydiacetylene Vesicles Induced by the Solvent Effect. *J. Phys. Chem. B* **2010**, *114*, 13365–13371.
- (26) Kang, D. H.; Jung, H.-S.; Ahn, N.; Lee, J.; Seo, S.; Suh, K.-Y.; Kim, J.; Kim, K. Biomimetic Detection of Aminoglycosidic Antibiotics using Polydiacetylene-Phospholipids Supramolecules. *Chem. Commun.* **2012**, *48*, 5313–5315.
- (27) Seo, S.; Lee, J.; Kwon, M. S.; Seo, D.; Kim, J. Stimuli-Responsive Matrix-Assisted Colorimetric Water Indicator of Polydiacetylene Nanofibers. *ACS Appl. Mater. Interfaces* **2015**, *7*, 20342–20348.
- (28) Lee, J.; Seo, S.; Kim, J. Colorimetric Detection of Warfare Gases by Polydiacetylenes Toward Equipment-Free Detection. *Adv. Funct. Mater.* **2012**, *22*, 1632–1638.
- (29) Lee, S.; Kim, J. Y.; Chen, X. Q.; Yoon, J. Recent Progress in Stimuli-Induced Polydiacetylenes for Sensing Temperature, Chemical and Biological Targets. *Chem. Commun.* **2016**, *52*, 9178–9196.
- (30) Davis, B. W.; Burris, A. J.; Niamnont, N.; Hare, C. D.; Chen, C. Y.; Sukwattanasinitt, M.; Cheng, Q. Dual-Mode Optical Sensing of Organic Vapors and Proteins with Polydiacetylene (PDA)-Embedded Electrospun Nanofibers. *Langmuir* **2014**, *30*, 9616–9622.
- (31) Kauffman, J. S.; Ellerbrock, B. M.; Stevens, K. A.; Brown, P. J.; Pennington, W. T.; Hanks, T. W. Preparation, Characterization, and Sensing Behavior of Polydiacetylene Liposomes Embedded in Alginate Fibers. *ACS Appl. Mater. Interfaces* **2009**, *1*, 1287–1291.
- (32) Park, M. K.; Kim, K. W.; Ahn, D. J.; Oh, M. K. Label-Free Detection of Bacterial RNA Using Polydiacetylene-Based Biochip. *Biosens. Bioelectron.* **2012**, *35*, 44–49.
- (33) Xu, Q.; Lee, S.; Cho, Y.; Kim, M. H.; Bouffard, J.; Yoon, J. A Polydiacetylene-Based Colorimetric and Fluorescent Chemosensor for the Detection of Carbon Dioxide. *J. Am. Chem. Soc.* **2013**, *135*, 17751–17754.
- (34) Jeon, H.; Lee, J.; Kim, M. H.; Yoon, J. Polydiacetylene-Based Electrospun Fibers for Detection of HCl Gas. *Macromol. Rapid Commun.* **2012**, *33*, 972–976.
- (35) Trachtenberg, A.; Malka, O.; Kootery, K. P.; Beglaryan, S.; Malferrari, D.; Galletti, P.; Prati, S.; Mazzeo, R.; Tagliavini, E.; Jelinek, R. Colorimetric Analysis of Painting Materials Using Polymer-Supported Polydiacetylene Films. *New J. Chem.* **2016**, *40*, 9054–9059.
- (36) Bheekhun, N.; Abu Talib, A. R.; Hassan, M. R. Aerogels in Aerospace: An Overview. *Adv. Mater. Sci. Eng.* **2013**, *2013*, 406065.
- (37) Ribeiro do Carmo, D.; Paim, L. L. Investigation about the Copper Adsorption on the Chloropropylsilica Gel Surface Modified with a Nanostructured Dendrimer DAB-Am-16: an Analytical Application for Determination of Copper in Different Samples. *Mater. Res.* **2013**, *16*, 164–172.
- (38) Volinsky, R.; Kolusheva, S.; Sheynis, T.; Kliger, M.; Jelinek, R. Glass-Supported Lipid/Polydiacetylene Films for Color Sensing of Membrane-Active Compounds. *Biosens. Bioelectron.* **2007**, *22*, 3247–3251.
- (39) Jiang, H.; Jelinek, R. Mixed Diacetylene/Octadecyl Melamine Nanowires Formed at the Air/Water Interface Exhibit Unique Structural and Colorimetric Properties. *Langmuir* **2015**, *31*, 5843–5850.
- (40) Sun, X. M.; Chen, T.; Huang, S. Q.; Li, L.; Peng, H. S. Chromatic Polydiacetylene with Novel Sensitivity. *Chem. Soc. Rev.* **2010**, *39*, 4244–4257.
- (41) Friedman, S.; Kolusheva, S.; Volinsky, R.; Zeiri, L.; Schrader, T.; Jelinek, R. Lipid/Polydiacetylene Films for Colorimetric Protein Surface-Charge Analysis. *Anal. Chem.* **2008**, *80*, 7804–7811.
- (42) Lifshitz, Y.; Upcher, A.; Kovalev, A.; Wainstein, D.; Rashkovsky, A.; Zeiri, L.; Golan, Y.; Berman, A. Zinc Modified Polydiacetylene Langmuir Films. *Soft Matter* **2011**, *7*, 9069–9077.
- (43) Wu, A. D.; Beck, C.; Ying, Y.; Federici, J.; Iqbal, Z. Thermochromism in Polydiacetylene-ZnO Nanocomposites. *J. Phys. Chem. C* **2013**, *117*, 19593–19600.
- (44) Lim, C.; Sandman, D. J.; Sukwattanasinitt, M. Topological Polymerization of tert-Butylcalix[4]arenes Containing Diynes. *Macromolecules* **2008**, *41*, 675–681.
- (45) Zhong, L.; Zhu, X. F.; Duan, P. F.; Liu, M. H. Photopolymerization and Formation of a Stable Purple Langmuir-Blodgett Film Based on the Gemini-Type Amphiphilic Diacetylene Derivatives. *J. Phys. Chem. B* **2010**, *114*, 8871–8878.
- (46) Yoon, J.; Chae, S. K.; Kim, J. M. Colorimetric Sensors for Volatile Organic Compounds (VOCs) Based on Conjugated Polymer-Embedded Electrospun Fibers. *J. Am. Chem. Soc.* **2007**, *129*, 3038–3039.
- (47) Jiang, H.; Wang, Y. L.; Ye, Q.; Zou, G.; Su, W.; Zhang, Q. J. Polydiacetylene-Based Colorimetric Sensor Microarray for Volatile Organic Compounds. *Sens. Actuators, B* **2010**, *143*, 789–794.
- (48) Hernandez, L. F.; Lima, R. D.; Tressino de Carvalho, A.; Demarquette, N. R.; Pereira da Silva, M. L. Plasma Polymerized Acetaldehyde Thin Films for Retention of Volatile Organic Compounds. *Quim. Nova* **2008**, *31*, 1410–1416.
- (49) Pattanatornchai, T.; Charoenthai, N.; Wacharasindhu, S.; Sukwattanasinitt, M.; Traiphol, R. Control Over the Color Transition Behavior of Polydiacetylene Vesicles Using Different Alcohols. *J. Colloid Interface Sci.* **2013**, *391*, 45–53.
- (50) Wu, A. D.; Gu, Y.; Tian, H. Q.; Federici, J. F.; Iqbal, Z. Effect of Alkyl Chain Length on Chemical Sensing of Polydiacetylene and Polydiacetylene/ZnO Nanocomposites. *Colloid Polym. Sci.* **2014**, *292*, 3137–3146.
- (51) Rakow, N. A.; Suslick, K. S. A Colorimetric Sensor Array for Odour Visualization. *Nature* **2000**, *406*, 710–713.